Chemical Science

EDGE ARTICLE

View Article Online
View Journal | View Issue

Check for updates

Cite this: *Chem. Sci.*, 2019, **10**, 497

All publication charges for this article have been paid for by the Royal Society of Chemistry

Open Access Article. Published on 15 October 2018. Downloaded on 5/12/2025 4:02:58 PM. This article is licensed under a Creative Commons Attribution 3.0 Unported Licence.

MoS_2-quantum dot triggered reactive oxygen species generation and depletion: responsible for enhanced chemiluminescence†

Xiangnan Dou, [ab] Qiang Zhang, [a] Syed Niaz Ali Shah, [a] Mashooq Khan,[a] Katsumi Uchiyama [b] and Jin-Ming Lin *[a]

Received 7th August 2018
Accepted 13th October 2018

DOI: 10.1039/c8sc03511c

rsc.li/chemical-science

Reactive oxygen species (ROS) generation is of intense interest because of its crucial role in many fields. Here we demonstrate that MoS_2-QDs exhibit a promising capability for the generation of reactive oxygen species, which leads to enhanced chemiluminescence. We discovered that the unique performance is due to hydroxyl radical activation increasing the active catalytic sites on molybdenum sulphide quantum dots (MoS_2-QDs). The reactive oxygen species, such as hydroxyl radicals ($^{\bullet}OH$), superoxide radicals ($^{\bullet}O_2^-$) and singlet oxygen ($^1O_2$) have been efficiently generated from H_2O_2 solution in alkaline conditions. In particular, the maximum $^{\bullet}OH$ yield was enhanced significantly (9.18 times) compared to the Fe(II)/H_2O_2 Fenton system under neutral conditions. These findings not only enrich our understanding of the fascinating performance of MoS_2 QDs, but also provide a new pathway for ROS generation in all kinds of pH environment.

Introduction

Reactive oxygen species (ROS) is a collective term for oxygen free radicals and molecules including superoxide radicals ($^{\bullet}O_2^-$), hydroxyl radicals ($^{\bullet}OH$) and singlet oxygen ($^1O_2$), which possess high reactivity compared to molecular O_2. Generation of abundant ROS is of immense interest in environmental and biological sciences.[1] To date, the ROS are usually generated using a photocatalytic process *via* light-activated photosensitizers or a chemical process *via* iron-mediated Fenton reaction.[2] However, the photocatalytic process suffers from undesirable bio-damage by ultra-violet (UV) radiation and low reactive oxygen species production. This has restricted the role of photocatalysis for biomedical applications.[3] The Fenton reaction can generate adequate ROS, however, this requires acidic conditions (pH = 3–4). Therefore, alternative reactions and conditions for ROS generation need to be pursued.

Nanoscale molybdenum sulphides (MoS_2) have gained widespread application in photo-responsive, energy storage and biosensor devices.[4] Besides, MoS_2 has been used as an excellent electro-catalyst for the hydrogen evolution reaction (HER).[5] However, the performance of molybdenum sulphide-quantum dots (MoS_2-QDs) toward chemiluminescence (CL) based on ROS generation has not been explored.

Here, we demonstrate the excellent capability of MoS_2-QDs to generate ROS from hydrogen peroxide in alkaline solution,

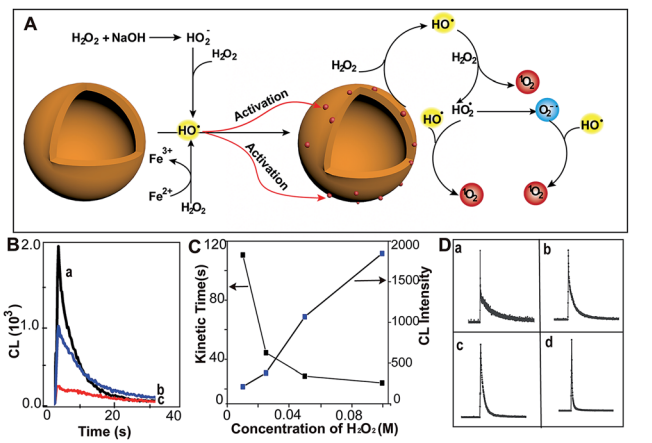

Fig. 1 MoS_2-QDs promote the generation of reactive oxygen species and induce chemiluminescence with H_2O_2 in alkaline conditions. (A) Schematic illustration of ROS generation by MoS_2-QDs. (B) The CL spectrum of injection order with (a) injection of MoS_2-QDs into a mixture of H_2O_2 + NaOH, (b) injection of NaOH into a mixture of H_2O_2 + MoS_2-QDs and (c) injection of H_2O_2 into a mixture of MoS_2-QDs + NaOH. (C) The dose-dependence of H_2O_2 concentration on kinetic decay time and CL intensity by injection of MoS_2-QDs into a H_2O_2–NaOH solution. (D) The CL kinetic curve at H_2O_2 concentrations of (a) 0.01, (b) 0.025, (c) 0.05, and (d) 0.1 M.

[a]*Beijing Key Laboratory of Microanalytical Methods and Instrumentation, MOE Key Laboratory of Bioorganic Phosphorus Chemistry & Chemical Biology, Department of Chemistry, Tsinghua University, Beijing, 100084, China. E-mail: jmlin@mail.tsinghua.edu.cn*

[b]*Department of Applied Chemistry, Graduate School of Urban Environmental Sciences, Tokyo Metropolitan University, Minamiohsawa, Hachioji, Tokyo 192-0397, Japan*

† Electronic supplementary information (ESI) available. See DOI: 10.1039/c8sc03511c

Open Access Article. Published on 15 October 2018. Downloaded on 5/12/2025 4:02:58 PM.
This article is licensed under a Creative Commons Attribution 3.0 Unported Licence.

which gives rise to CL emission (Fig. 1A). The hydroxyl radicals (˙OH) from intrinsic reactions such as H_2O_2 in alkaline medium and the Fe(II)/H_2O_2 Fenton system activate MoS_2-QDs and generate active catalytic sites on their surface. These active sites then facilitate the conversion of H_2O_2 to generate a sufficient amount of ROS, which leads to a strong CL-emission.

Results and discussion

The MoS_2-QDs were prepared by solvothermal treatment in *N*,*N*-dimethylformamide (DMF), as proposed by Wang *et al.*[6] The MoS_2-QDs exhibited an average size of ~3.7 nm (Fig. S1, ESI†). The as-prepared product (0.9 mg ml^{-1}) was dispersed in water and a transparent pale-yellow solution was obtained, which exhibited a strong fluorescence emission over a wide range of excitation wavelengths (Fig. S2, ESI†).

The chemiluminescence (CL) was produced by MoS_2-QDs and H_2O_2. A stronger CL was obtained with injection of the MoS_2-QD suspension into a pre-mixed H_2O_2/NaOH solution, whereas those with the addition of H_2O_2 to NaOH/MoS_2-QDs or with the addition of NaOH to H_2O_2/MoS_2-QDs, exhibited relatively weaker CL-emission (Fig. 1B). We found that the CL was not only correlated to the injection order, but also to the NaOH concentration. The CL intensity was found to increase with increasing concentration of NaOH and no CL emission was found under acidic or neutral conditions. This was attributed to the remarkable decomposition of H_2O_2 in alkaline medium[7] (80% and 15% at pH = 13 and 10.5 respectively) (Fig. S3, ESI†). The results suggested that the decomposition of H_2O_2 plays an important role in the enhanced CL-emission with the addition of MoS_2-QDs. The hydroxyl radical (˙OH) generation from H_2O_2 in the presence of base is given in eqn (1) and (2). Perhydroxyl ions (HO_2^-) were formed through the decomposition of H_2O_2 in base; then the HO_2^- reacted with undissociated H_2O_2 molecules to produce hydroperoxide radicals (HO_2˙) and ˙OH.[8]

$$H_2O_2 + OH^- \rightarrow H_2O + HO_2^- \quad (1)$$

$$HO_2^- + H_2O_2 \rightarrow HO_2^{\cdot} + {}^{\cdot}OH + OH^- \quad (2)$$

Ouyang *et al.* have reported that intrinsic defects can be generated to activate and increase the number of catalytic sites on MoS_2.[9] The ˙OH is a strong oxidizing agent, which has a redox potential of 2.8 V,[10] therefore, the production of ˙OH leads to radical attack on the MoS_2-QDs and generates defects. This increases the effective catalytic sites of the MoS_2-QDs and hence facilitates the further decomposition of H_2O_2. The occurrence of defects was evidenced by the short lifetime of about 5.2 ns of the MoS_2-QDs (Fig. S4, ESI†). To clarify the role of ˙OH in the strong CL-emission of the MoS_2-QD/H_2O_2 system, experiments with H_2O_2 at different concentrations were performed. We found that the CL-emission intensity of the MoS_2-QD/H_2O_2 system is dependent on the concentration of H_2O_2 (Fig. 1C). With increasing [H_2O_2] from 0.01 M to 0.1 M, the intensity of CL increased progressively. The CL kinetic decay time was also found to be dependent on the H_2O_2 concentration. A flash CL-emission was observed at high H_2O_2 concentration (0.1 M), whereas a relatively slower decay was observed at low concentration (Fig. 1D).

Electron Spin Resonance (ESR) spectroscopy was performed to directly examine the generation of ˙OH under different H_2O_2 conditions. A larger yield of ˙OH was observed as [H_2O_2] was increased (Fig. 2A(a) and B(a)). This provides clear evidence that activation of the MoS_2-QDs is highly dependent on ˙OH formation. No obvious ESR signals for DMPO–OH were observed without MoS_2-QDs, while the ˙OH was significantly enhanced in the presence of activated MoS_2-QDs at [H_2O_2] = 0.01 M in NaOH (0.1 M) (Fig. 2A(b)). In addition, we found the signal for DMPO–OH and DMPO–$^{\cdot}O_2^-$ (ref. 11) in the presence of MoS_2-QDs is stronger than that in the absence of MoS_2-QDs at H_2O_2 = 0.1 M in NaOH (0.1 M) (Fig. 2B(b)). These results suggest the dependence of ˙OH generation on H_2O_2 concentration and the ability of the MoS_2-QDs for ROS generation, which leads to the strong CL-emission of the MoS_2-QD/H_2O_2 system.

Moreover, the UV-vis spectra (Fig. 2C) with nitrotetrazolium blue chloride (NBT) as a superoxide radical ($^{\cdot}O_2^-$) probe[12] and ESR spectra (Fig. 2D) with 2,2,6,6-tetramethyl-4-piperidine (TEMP) as a singlet oxygen ($^1O_2$) probe[13] also showed a significant increase in $^{\cdot}O_2^-$ and $^1O_2$ production in the presence of MoS_2-QDs. The generation pathways of $^{\cdot}O_2^-$ and $^1O_2$ *via* radical reactions are given in eqn (3)–(7).[14,15] We hypothesized that the active sites induced by ˙OH were responsible for the generation of ˙OH, $^{\cdot}O_2^-$, and $^1O_2$ by facilitating the conversion of H_2O_2 into more ROS.

$$^{\cdot}OH + H_2O_2 \rightarrow HO_2^{\cdot} + H_2O \quad (3)$$

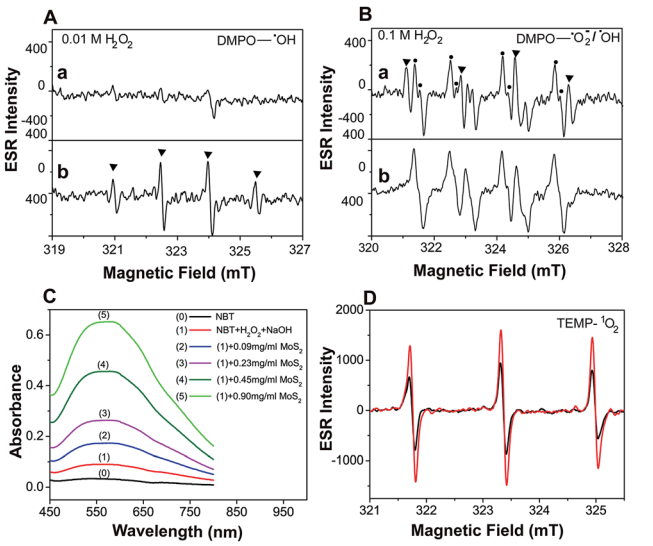

Fig. 2 Evaluation of the enhancement of ˙OH, $^{\cdot}O_2^-$ and $^1O_2$ production by MoS_2-QDs in the H_2O_2–NaOH system. (A) ESR spectrum of 5,5-dimethyl-1-pyrroline *N*-oxide (DMPO) with ˙OH obtained from 0.01 M H_2O_2 in 0.1 M NaOH (a), and the same as the above conditions but with MoS_2-QDs (b). (B) ESR spectrum of DMPO with ˙OH or $^{\cdot}O_2^-$ obtained from 0.1 M H_2O_2 in 0.1 M NaOH (a), and the same as the above conditions but with MoS_2-QDs (b). (C) The absorbance of NBT in the H_2O_2–NaOH system with the addition of MoS_2-QDs. (D) ESR spectrum of TEMP with $^1O_2$ production from H_2O_2–NaOH (black) and MoS_2-QDs–H_2O_2–NaOH (red).

This journal is © The Royal Society of Chemistry 2019

Open Access Article. Published on 15 October 2018. Downloaded on 5/12/2025 4:02:58 PM.
This article is licensed under a Creative Commons Attribution 3.0 Unported Licence.

$$HO_2^{\cdot} + OH^- \rightarrow {}^{\cdot}O_2^- + H_2O \quad (4)$$

$$\cdot OH + \cdot OH \rightarrow H_2O + \frac{1}{2}(O_2 + {}^1O_2) \quad (5)$$

$$^{\cdot}OH + HO_2^{\cdot} \rightarrow H_2O + O_2 + {}^1O_2 \quad (6)$$

$$^{\cdot}OH + {}^{\cdot}O_2^- \rightarrow OH^- + {}^1O_2 \quad (7)$$

In order to further evaluate the dependence of MoS_2-QD activation and CL-emission on the generation and concentration of $^{\cdot}OH$, a classic $^{\cdot}OH$ generation Fenton system was investigated. We found that, MoS_2-QDs strongly enhanced the CL-emission of the Fe^{2+}/H_2O_2 system. It was striking that equivalent CL-emission was produced under both neutral and acidic conditions (Fig. 3A). Besides, $^{\cdot}OH$ generation was significantly accelerated and compared to the Fe^{2+}/H_2O_2 system, a 9.18 times greater yield of $^{\cdot}OH$ was observed (Fig. 3B). These results confirmed the hypothesis of ROS generation through $^{\cdot}OH$-activated MoS_2-QDs.

To further verify the generation of $^{\cdot}OH$, the Fenton-oxidation of tetramethylbenzidine (TMB) was introduced, which is known to be oxidized by $^{\cdot}OH$.[16] In the absence of MoS_2-QDs, TMB was oxidized slowly and reached a maximum absorbance intensity ($\lambda_{max} = 652$ nm) after 60 s. Nevertheless, in presence of MoS_2-QDs, a rapid strong absorbance at 652 nm was observed (Fig. S5, ESI†), indicating a rapid formation of the bluish oxidized TMB because of $^{\cdot}OH$ being generated in large amounts. This confirmed that MoS_2-QD driven Fenton reaction can effectively produce $^{\cdot}OH$.

The generation of $^{\cdot}OH$ can effectively degrade organic contaminants.[17] Therefore, phenol, pyrocatechol, rhodamine B (RhB) and methylene blue (MB) were used to find the degradation efficiency and fate of $^{\cdot}OH$ in the Fenton (Fe^{2+}/H_2O_2) and MoS_2-QD supported Fenton system. Phenolic compound concentrations were measured by using 4-aminoantipyrine for the colorimetric determination.[18] As expected, a significant decrease of phenol and pyrocatechol (Fig. S6, ESI†) was observed when phenol or pyrocatechol were incubated with the MoS_2-QD supported Fe^{2+}/H_2O_2 system as compared to the traditional Fe^{2+}/H_2O_2 Fenton system, indicating a higher degradation efficiency for phenolic compounds with the Fe^{2+}/H_2O_2–MoS_2-QD system. In addition, the degradation of RhB and MB has been detected by the UV-visible method. In the presence of MoS_2-QDs, MoS_2-QDs were found to significantly inhibit both RhB and MB degradation efficiency (Fig. 4). Moreover, the presence of MoS_2-QDs showed a more negative influence on MB degradation, inhibiting the efficiency of MB degradation by 72%, as well as that of RhB degradation efficiency by 8%. This difference towards RhB and MB degradation is probably attributable to the lower reactivity of MB compared to RhB in the Fe^{2+}/H_2O_2–MoS_2-QD system, because of significant structural differences between the two different organic fractions (RhB and MB). It has been found previously that $^{\cdot}OH$ could be consumed by injection of holes into semiconductor nano-materials.[19] The selective degradation of phenolic compounds as compared to RhB and MB is probably due to the higher reaction rate of $^{\cdot}OH$ with phenolic compounds ($k \approx 10^{10}$ M^{-1} s^{-1}),[20] which makes phenolic compounds more competitive for reacting with $^{\cdot}OH$ rather than MoS_2-QDs in the degradation process. In contrast, $^{\cdot}OH$ reacts with MoS_2-QDs preferentially rather than the aromatic heterocyclic compounds, such as RhB and MB, due to the one order of magnitude lower rate ($k \approx 10^9$ M^{-1} s^{-1}).[21] These results strongly indicated that a rapid reaction of MoS_2-QDs with $^{\cdot}OH$ (and $^{\cdot}O_2^-$) forming hole-injection ($(MoS_2)^{\cdot+}$ QDs) and electron-injection ($(MoS_2)^{\cdot-}$ QDs) species (eqn (8) and (9)) occurred.

$$MoS_2\text{-QDs} + {}^{\cdot}OH \rightarrow (MoS_2)^{\cdot+}\ QDs + OH^- \quad (8)$$

$$MoS_2\text{-QDs} + {}^{\cdot}O_2^- \rightarrow (MoS_2)^{\cdot-}\ QDs + O_2 \quad (9)$$

The annihilation of $(MoS_2)^{\cdot+}$ and $(MoS_2)^{\cdot-}$ resulted in energy release in the form of CL emission,[22] which has been clarified

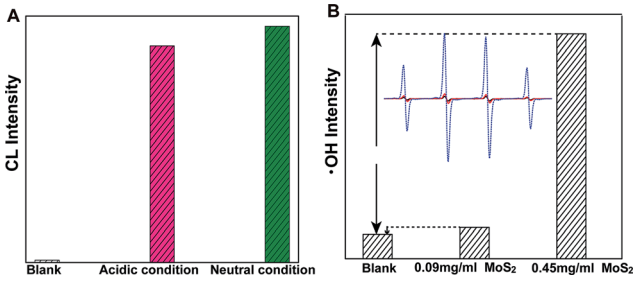

Fig. 3 Enhancement of chemiluminescence and hydroxyl radical ($^{\cdot}OH$) production by MoS_2-QDs in the Fe^{2+}–H_2O_2 system (A) the chemiluminescence of Fe^{2+}–H_2O_2 (blank); and the CL produced by the addition of MoS_2-QDs to the Fe^{2+}–H_2O_2 system under acidic (pH = 3.7) and neutral conditions. (B) The hydroxyl radicals generated from Fe^{2+}–H_2O_2 (blank) and from the addition of MoS_2-QDs with a concentrations of 0.09 mg ml^{-1} and 0.45 mg ml^{-1}. The inset in panel B is the ESR spectrum of DMPO with $^{\cdot}OH$ generated from Fe^{2+}–H_2O_2 (black) and with the addition of MoS_2-QDs with concentrations of 0.09 mg ml^{-1} (red) and 0.45 mg ml^{-1} (blue).

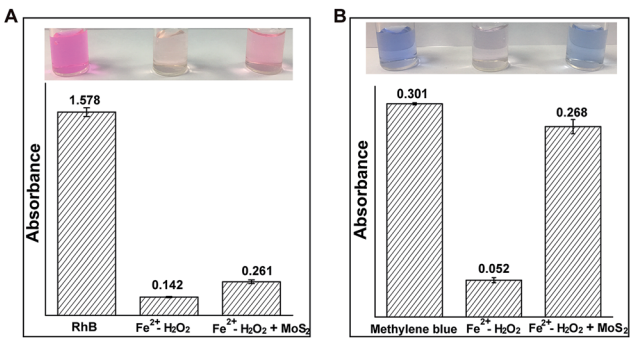

Fig. 4 The influence of MoS_2-QDs on organic contaminant degradation in the Fe^{2+}–H_2O_2 Fenton system. (A) The absorbance of rhodamine B at 554 nm in the Fe^{2+}–H_2O_2 and Fe^{2+}–H_2O_2 + MoS_2-QD systems; (B) the absorbance of methylene blue at 626 nm in the Fe^{2+}–H_2O_2 and Fe^{2+}–H_2O_2 + MoS_2-QD systems. The solution conditions were 0.01 M H_2O_2, 0.45 mg ml^{-1} MoS_2-QDs, 1 mM Fe^{2+}, 5 μg ml^{-1} RhB and 5 μg ml^{-1} MB.

Open Access Article. Published on 15 October 2018. Downloaded on 5/12/2025 4:02:58 PM. This article is licensed under a Creative Commons Attribution 3.0 Unported Licence.

through a CL-emission spectrum. The CL emission spectrum was centered at 490 nm and 550 nm, which may contain overlap of $^1O_2$ and MoS_2 emission[23] (Fig. S7, ESI†). To verify that this emission was from the recombination of $(MoS_2)^{\bullet+}$ and $(MoS_2)^{\bullet-}$ and not from the overlap of $^1O_2$ and MoS_2-QD emission, the CL-emission was recorded in D_2O as a solvent instead of H_2O, because $^1O_2$ possesses a 13 times longer lifetime in D_2O than in H_2O.[24] Generally, if the CL emission originated from $^1O_2$, one would expect alteration of the kinetic reaction in D_2O. However, no obvious change was observed, indicating no contribution of the $^1O_2$ to the CL-emission due to the annihilation of electron–hole combination of $(MoS_2)^{\bullet+}$ QDs and $(MoS_2)^{\bullet-}$ QDs (Fig. S8, ESI†).

Conclusions

For the first time, we have demonstrated the excellent capability of MoS_2-QDs toward ROS generation. We explored that the synergistic effect of enhanced ROS production and ROS depletion were the main factors leading to the CL-emission of MoS_2-QDs with H_2O_2 in alkaline medium; and with the Fenton reagent under neutral and acidic conditions. These findings present a new pathway for ROS generation over the whole pH-range. Thus, MoS_2-QDs have potential applications for degradation of organic pollutants and chemo-dynamic therapy.

Conflicts of interest

There are no conflicts to declare.

Acknowledgements

This work was supported by the National Natural Science Foundation of China (Nos. 21435002, 21621003) and JSPS RONPAKU (Ph.D. Dissertation) Program.

References

1 (*a*) H. Wang, S. Jiang, W. Shao, X. Zhang, S. Chen, X. Sun, Q. Zhang, Y. Luo and Y. Xie, *J. Am. Chem. Soc.*, 2018, **140**, 3474–3480; (*b*) R. C. Gilson, L. C. L. Black, D. D. Lane and S. Achilefu, *Angew. Chem., Int. Ed.*, 2017, **129**, 10857–10860; (*c*) J. Bai, X. D. Jia, W. Zhen, W. Cheng and X. Jiang, *Angew. Chem., Int. Ed.*, 2018, **140**, 106–109.

2 (*a*) Y. Li, W. Zhang, J. F. Niu and Y. S. Chen, *ACS Nano*, 2012, **6**, 5164–5173; (*b*) C. Yang, W. Dong, G. Cui, Y. Zhao, X. Shi, X. Xia, B. Tang and W. Wang, *RSC Adv.*, 2017, **7**, 23699–23708; (*c*) Y. Zheng, D. Zhang, S. Shah, H. Li and J. Lin, *Chem. Commun.*, 2017, **53**, 5657–5660.

3 (*a*) S. Shah, L. Lin, Y. Zheng, D. Zhang and J. Lin, *Phys. Chem. Chem. Phys.*, 2017, **19**, 21604–21611; (*b*) C. Zhang, W. Bu, D. Ni, S. Zhang, Q. Li, Z. Yao, J. Zhang, H. Yao, Z. Wang and J. Shi, *Angew. Chem., Int. Ed.*, 2016, **55**, 2101–2106.

4 (*a*) O. Sanchez, D. Lembke, M. Kayci, A. Radenovic and A. Kis, *Nat. Nanotechnol.*, 2013, **8**, 497–501; (*b*) Y. Lin, D. Dumcenco, Y. Huang and K. Suenaga, *Nat. Nanotechnol.*, 2014, **9**, 391–396; (*c*) C. Zhu, Z. Zeng, H. Li, F. Li, C. Fan and H. Zhang, *J. Am. Chem. Soc.*, 2013, **135**, 5998–6001.

5 (*a*) G. Li, D. Zhang, Y. Yu, S. Huang, W. Yang and L. Cao, *J. Am. Chem. Soc.*, 2017, **139**, 16194–16200; (*b*) Y. Shi, Y. Zhou, D. Yang, W. Xu, C. Wang, F. Wang, J. Xu, X. Xia and H. Chen, *J. Am. Chem. Soc.*, 2017, **139**, 15479–15485; (*c*) X. Zhao, H. Zhu and X. Yang, *Nanoscale*, 2014, **6**, 10680–10685.

6 J. Wang, X. Tan, X. Pang, L. Liu, F. Tan and N. Li, *ACS Appl. Mater. Interfaces*, 2016, **8**, 24331–24338.

7 O. Spalek, J. Balej and I. Pasek, *J. Chem. Soc., Faraday Trans. 1*, 1982, **78**, 2349–2359.

8 A. Hebeish, A. Bayazeed, B. I. Abdel Gawad, S. K. Basily and S. El-Bazza, *Starch*, 1984, **10**, 344–349.

9 Y. Ouyang, C. Ling, Q. Chen, Z. Wang, L. Shi and J. Wang, *Chem. Mater.*, 2016, **28**, 4390–4396.

10 L. Kong, G. Fang, Y. Kong, M. Xie, V. Natarajan, D. Zhou and J. Zhan, *J. Hazard. Mater.*, 2018, **357**, 109–118.

11 N. Zhou, T. Qiu, L. Ping and L. Yang, *Magn. Reson. Chem.*, 2006, **44**, 38–44.

12 K. Reybier, S. Ayala, B. Alies, J. V. Rodrigues, S. B. Rodriguez, G. Penna, F. Collin, C. M. Gomes, C. Hureau and P. Faller, *Angew. Chem., Int. Ed.*, 2016, **55**, 1085–1089.

13 Y. Zheng, X. Dou, H. Li and J.-M. Lin, *Nanoscale*, 2016, **8**, 4933–4937.

14 I. Ivanova, S. Trofimova, I. Piskarev, N. Aristova, O. Burhina and O. Soshnikova, *J. Biophys. Chem.*, 2012, **3**, 88–100.

15 Z. Lin, H. Chen, Y. n. Zhou, N. Ogawa and J.-M. Lin, *J. Environ. Sci.*, 2012, **24**, 550–557.

16 W. Zhang, S. Hu, J. Yin, W. He, W. Lu, M. Ma, N. Gu and Y. Zhang, *J. Am. Chem. Soc.*, 2016, **138**, 5860–5865.

17 W. Zhang, Y. Su, X. Zhang, Y. Yang and X. Guo, *RSC Adv.*, 2016, **6**, 64626–64633.

18 E. Munaf, R. Zein, R. Kurniadi and I. Kurniadi, *Environ. Technol.*, 1997, **18**, 355–358.

19 Y. Li, Y. Zheng, D. Zhang, H. Li, Y. Ma and J. M. Lin, *Chin. Chem. Lett.*, 2017, **28**, 184–188.

20 G. Buxton, C. Greenstock, W. Helman and A. B. Ross, *J. Phys. Chem. Ref. Data*, 1988, **17**, 513–861.

21 W. Haag and C. Yao, *Environ. Sci. Technol.*, 1992, **26**, 1005–1013.

22 B. Chen, F. Wang, W. Yao, Z. Lin, X. Zhang, S. Luo, L. Zheng and X. Lin, *Anal. Methods*, 2018, **10**, 474–480.

23 W. Adam, D. V. Kazakov and V. P. Kazakov, *Chem. Rev.*, 2005, **105**, 3371–3387.

24 R. Huang, E. Choe and D. B. Min, *J. Food Sci.*, 2004, **69**, 726–732.

 This journal is © The Royal Society of Chemistry 2019